ANNALS OF GEOPHYSICS, 69, 5, A548, 2026; doi:10.4401/ag-9531
OPEN ACCESS

# Evaluating the impact of a tilted eccentric dipole model on ionospheric simulations over the South American sector under quiet geomagnetic conditions

Valentín Venchiarutti[*,1], Blas F. de Haro Barbás[1,2], Jonas R. Souza[3], Manuel Bravo[4], Ângela M. Santos[3], Ana G. Elias[1,2]

(1) Universidad Nacional de Tucumán, Facultad de Ciencias Exactas y Tecnología, Departamento de Física, Tucumán, Argentina
(2) INFINOA (CONICET-UNT) Argentina
(3) Instituto Nacional de Pesquisas Espaciais, INPE, São José dos Campos, SP, Brazil
(4) Centro de Instrumentación Científica, Universidad Adventista de Chile, Chillán, Chile

Article history: received January 8, 2026; accepted July 8, 2026

## Abstract

This work presents the first comprehensive evaluation of the SUPIM-INPE ionospheric model using the tilted eccentric dipole (ED) magnetic field configuration, compared with the tilted centered dipole (CD), and validated against observational data of the F2-layer critical frequency (foF2) that is a key parameter for understanding ionospheric behavior. Simulations were carried out using two ED configurations: one implemented in single precision and the other in double precision to minimize computational rounding and truncation errors and improve numerical stability. Both configurations were tested over five ionospheric stations across South America: Belém (1.43°S, 48.44°W), São Luís (2.60°S, 44.20°W), Cachoeira Paulista (22.70°S, 45.00°W), Tucumán (26.90°S, 65.40°W), and Santa Maria (29.73°S, 53.80°W). Model outputs were compared with ionosonde data from these stations for geomagnetically quiet days during both high (18 January 2014 and 9 May 2024) and moderate (7 and 31 January 2014, 30 January 2023, 21 and 22 April 2023) solar activity conditions. Model performance was evaluated using the Mean Absolute Error (MAE), Mean Relative Error (MRE), and the coefficient of determination ($R^2$). Our results indicate that the double-precision ED configuration achieves better agreement with observations, highlighting the importance of both a more realistic representation of the geomagnetic field and the reduction of numerical errors in magnetic field geometry and coordinate transformation routines.

Keywords: Ionosphere; SUPIM-INPE; foF2; Double precision; Tilted eccentric dipole

## 1. Introduction

The original Sheffield University Plasmasphere-Ionosphere Model (SUPIM) is a computer model written in FORTRAN (Bailey and Sellek, 1990) and has been developed over the past decades (Bailey et al., 1993, 1997;

Bailey and Balan, 1996; Souza et al., 2000) with magnetic field configuration options such as axial dipole, tilted centered dipole, and tilted eccentric dipole. In the present work, a modified version of SUPIM at the National Institute for Space Research, called SUPIM-INPE, is used in order to make the tilted eccentric dipole option fully operational. This was achieved by implementing new and modified algorithms in the section of the code related to Earth's magnetic field.

In the model, the time-dependent continuity, momentum and energy balance equations describing the chemical and physical processes of the Earth's mid- and low-latitude ionosphere and plasmasphere are solved along closed dipole magnetic field lines between altitudes of around 110 km in both hemispheres to give values for the densities, field-aligned velocities and temperatures of $O^+$, $H^+$, $He^+$, $O_2{}^+$, $N_2{}^+$ and $NO^+$ ions, and electrons. The SUPIM-INPE (axial dipole and tilted centered dipole) extends the calculations along the magnetic field lines from its original lower apex and base altitude limits from 150 km and 110 km (Bailey et al., 1993; Bailey and Balan, 1996) down to 90 and 80 km, respectively, and adds the calculations for a seventh ion $N^+$ (Santos et al., 2005, Souza et al., 2010, 2013 and Santos et al., 2016a,b; Lomotey et al., 2024). In addition, the chemical reaction scheme from Huba et al. (2000), which is prepared to include the E region, has been used. The photochemical equilibrium condition was applied only at the base altitudes, whereas the original SUPIM uses this condition for the entire E layer. The main input parameters to this model are the neutral wind, the neutral densities, the ionizing solar radiation (EUV flux), the solar index flux (F10.7), and equatorial vertical drift $E \times B$. The neutral winds and densities are obtained from the Horizontal Wind Model 2014 (HWM14, Drob et al., 2015) and NRLMSISE-00 (Picone et al., 2002), respectively. The EUV flux models developed by Richards et al. (2006, 2010), and the vertical $E \times B$ drift velocities by Scherliess and Fejer (1999) were implemented.

SUPIM-INPE uses two Earth's magnetic field models in its basic form, namely, axial centered dipole, and tilted centered dipole (CD). In this study, the tilted eccentric dipole (ED) option has been implemented, and the analysis is restricted to the comparison between the CD and ED configurations. While the axial centered dipole model uses one Gauss coefficient ($g_1^0$) from the IGRF-14 model, CD and ED models use three ($g_1^0$, $g_1^1$, $h_1^1$) and eight ($g_1^0, g_1^1, h_1^1, g_2^0, g_2^1, g_2^2, h_2^1, h_2^2$) Gauss coefficients respectively. The ED model consists of a magnetic dipole with its axis parallel to the axis of the tilted centered dipole but with its center displaced from the center of the Earth (Koochak and Fraser-Smith, 2017). In addition, the ED model calculates the change from geographic to magnetic coordinates, and vice versa, by means of the corresponding subroutine, using the equations given by Fraser-Smith in SUPIM-INPE. These equations allow extending the calculations along the magnetic field lines from its original lower apex and base altitude limits of 150 km and 140 km (Fraser-Smith, 1987). This dipole model is called Schmidt eccentric dipole (Schmidt, 1934).

This work aims to compare and validate the responses of SUPIM-INPE obtained with the CD and ED magnetic field configurations, improving the reliability of ionospheric variability studies and comparisons with experimental measurements. This makes it a valuable tool for the scientific community in investigating ionospheric dynamics and their effects on radio signal propagation in the magnetic configuration of an eccentric dipole. Our goal is to evaluate the performance of SUPIM-INPE with the ED configuration in predicting F2-layer critical frequency (foF2). Single and double precision were used in routines related to the geometry of magnetic field lines and conversion of geographic to magnetic coordinates, and a comparison was made also with the CD configuration using observational ionosonde data over South America. This work shows a quantitative assessment of the improvements obtained by adopting an ED geometry and by enhancing numerical precision. As a result, advantages of a more realistic foF2 modeling in areas with a particular magnetic field configuration, such as South America, are shown in this study.

The ionospheric stations used in this work are of particular importance because they are located within or near the region affected by the South Atlantic Magnetic Anomaly (SAMA). This geomagnetic anomaly is characterized by a weakened magnetic field intensity relative to other longitudes, which enhances particle precipitation and alters the morphology and dynamics of the low-latitude ionosphere (Abdu et al., 1973, 1985, 2005; Batista and Abdu, 1977; Da Silva et al., 2022). Under quiet geomagnetic conditions ($Ap < 10$ nT), the ionosphere in SAMA-affected regions becomes particularly sensitive to the intrinsic configuration of the geomagnetic field, making these stations an ideal observational framework for assessing how the ED formulation improves the SUPIM-INPE model relative to the CD configuration. In this work, quiet conditions are intentionally selected to isolate the effects of magnetic field geometry. Their spatial distribution across the Brazilian sector also provides a representative latitudinal sampling of SAMA, enabling a robust evaluation of foF2 variability and isolating more clearly the impact of magnetic field geometry on quiet-time ionospheric behavior.

# 2. Experimental data, model calculations, and Comparison Methods

## 2.1 F2-layer critical frequency experimental data

To validate this new version of the model, data from stations located in the southern region of America were used as mentioned above. These stations provide foF2 data every 5 to 15 minutes. Quiet days with low geomagnetic activity index (Ap < 10 nT) and periods of moderate to high solar activity were selected, defined according to daily F10.7 values between 100 and 180 solar flux units (s.f.u.) for moderate activity and above 180 s.f.u. for high activity level, where 1 s.f.u. = $10^{-22}$ W $m^{-2}$ $Hz^{-1}$. Table 1 summarizes the observation days, stations, and corresponding solar and geomagnetic conditions used in this study.

**Table 1.** Observation Days, Stations, and Solar/Geomagnetic Conditions.

| Dates | Stations | F10.7 (s.f.u.) | F10.7A (81 days, s.f.u.) | Solar Condition | Daily Ap (nT) |
|---|---|---|---|---|---|
| 7 Jan 2014 | Tucumán | 154.3 | 149.8 | Moderate | 7.0 |
| 18 Jan 2014 | Tucumán | 229.3 | 152.4 | High | 1.0 |
| 31 Jan 2014 | Tucumán | 125.5 | 155.6 | Moderate | 1.0 |
| 30 Jan 2023 | Santa Maria | 135.9 | 131.9 | Moderate | 4.0 |
| 21 Apr 2023 | Belém, São Luís, Cachoeira Paulista, Santa Maria | 152.7 | 151.7 | Moderate | 9.0 |
| 22 Apr 2023 | Cachoeira Paulista, Santa Maria | 142.7 | 151.9 | Moderate | 6.0 |
| 9 May 2024 | Belém, São Luís | 237.7 | 178.8 | High | 5.0 |

The Tucumán station (TUC20, 26.90°S, 65.40°W, dip ≈ −30º) operates an AIS-INGV ionosonde (Zuccheretti et al., 2003), managed by the Tucumán Space Weather Center (https://spaceweather.facet.unt.edu.ar/), at the Facultad de Ciencias Exactas y Tecnología (FACET), Universidad Nacional de Tucumán (UNT), Argentina. The system performs vertical soundings in the 2-20 MHz frequency range, with a typical time interval of 10 minutes, generating standard ionograms (Zuccheretti et al., 2003; Molina et al., 2013). For this station, all ionograms were manually scaled to ensure consistent identification of the ionospheric layers.

For the remaining stations – Santa Maria (SMK29, 29.73°S, 53.80°W, dip ≈ −37°), Belém (BLJ03, 1.43°S, 48.44°W, dip ≈ −7°), Cachoeira Paulista (CXP, 22.70°S, 45.00°W, dip ≈ −35°), and São Luís (SLZ, 2.60°S, 44.20°W, dip ≈ −8°) – the ionospheric parameters were derived from Digisonde Portable Sounder 4D (DPS-4D) systems (Reinisch et al., 2009). These digital ionosondes operate in the high-frequency 3-30 MHz band. The SMK29 system offers a temporal resolution of 5 minutes and a height resolution of approximately 2.5 km, typical of DPS-4D sounders. Because the system supports multi-beam off-vertical sounding, the ionograms may include echoes from oblique propagation paths (Resende et al., 2024).

For these stations, ionospheric parameters were initially preprocessed using the ARTIST software (Automatic Real-Time Ionogram Scaler with True Height) (Reinisch and Huang,1983; Reinisch et al., 2005) and were subsequently manually edited using the SAO-Explorer software to ensure the reliability of the derived parameters.

## 2.2 SUPIM-INPE calculations

SUPIM-INPE calculations were performed for the stations and conditions listed in Table 1 for two different geomagnetic field configurations: CD and ED. In the ED case, its implementation used the transformation equations

between geographic and magnetic coordinates, including the displacement of the dipole with respect to the Earth's center, according to Fraser-Smith (1987), based on the classic work of Cole (1963).

For this work, we developed two versions of the ED model: one using implicit double precision (SUPIM-INPE ED_IDP) and another using explicit double precision (SUPIM-INPE ED_EDP) in the routines that define the geometry of the magnetic field lines. Both versions were compiled with ifort -r8, which promotes single precision variables to implicit double precision. However, since trigonometric functions are still evaluated in single precision before being promoted, rounding and truncation errors arise and propagate through each iteration.

Although automatic promotion ensures 64-bit storage of variables, it does not necessarily guarantee full numerical equivalence with an implementation explicitly defined in double precision. In nonlinear coordinate transformations and iterative calculations, small rounding differences may propagate and influence convergence behavior. By rewriting these routines with explicit double precision, we minimized the accumulation of rounding and truncation errors in the iterative calculations, thereby improving numerical accuracy and physical consistency.

The CD configuration corresponds to the standard implementation of SUPIM-INPE. It is written using single precision declarations and compiled with automatic double precision promotion (ifort -r8), consistent with its operational use. Unlike the ED configuration, no explicitly redefined double precision version was developed for CD in this study; therefore, the IDP versus EDP comparison applies exclusively to the ED framework.

### 2.3 Validation metrics

To quantitatively evaluate the performance of each model, three statistical comparative metrics were estimated by comparing each SUPIM-INPE configuration results with the experimental foF2 data. They are the Mean Absolute Error (MAE), the Mean Relative Error (MRE), and the Coefficient of Determination ($R^2$), defined by:

$$MAE = \frac{1}{N}\sum_{i=1}^{N}\left|y_{measured,i} - y_{model,i}\right| \tag{1}$$

$$MRE = \frac{1}{N}\sum_{i=1}^{N}\frac{y_{measured,i} - y_{model,i}}{y_{measured,i}} \times 100 \tag{2}$$

$$R^2 = 1 - \frac{\sum_{i=1}^{N}\left(y_{measured,i} - y_{model,i}\right)^2}{\sum_{i=1}^{N}\left(y_{measured,i} - y_{measured\ mean}\right)^2} \tag{3}$$

where $y_{measured,i}$ correspond to foF2 obtained from the ionospheric stations and $y_{model,i}$ corresponds to foF2 values modeled by SUPIM-INPE with ED (IDP and EDP) and with CD. The quantities $y_{measured\ mean}$ and $y_{model\ mean}$ represent the arithmetic means of the measured and modeled foF2 values. N is the total number of observations.

MRE measures the average bias of modeled foF2 values over or underestimating measured values, depending on its sign: negative or positive, respectively. In this case, it is multiplied by 100, so it gives the percentage bias, and its optimal value is zero. MAE is a scale-dependent measure of deviation that, in this case, corresponds to modeled data deviation from measurements. The optimal value is zero, indicating that both foF2 data series are identical.

$R^2$ measures the proportion of the variance in the experimental foF2 data explained by the model relative to the observational mean. The maximum possible value is 1, indicating a perfect fit between model predictions and observations. An $R^2$ value of 0 indicates that the model is not more skillful than the observational mean, whereas negative values indicate that the model predictions are less accurate than simply using the mean of the observations.

MAE, MRE, and $R^2$ values have been assessed for each day and station listed in Table1.

## 3. Results and Discussion

Figures 1-5 present foF2 values as a function of UT for the studied periods, including the experimental observations and the SUPIM-INPE model results obtained with the ED-IDP, ED-EDP and CD configurations. Each figure corresponds

to a single station and includes all available days for that station; therefore, the number of panels may vary among figures. The figures are ordered according to station latitude, from the northernmost to the southernmost site: Belém, São Luís, Cachoeira Paulista, Tucumán, and Santa María. The SUPIM-INPE CD configuration (green dots) corresponds to the version most commonly used by the scientific community, whereas this study presents, for the first time, results obtained with the SUPIM-INPE ED configuration (blue dots for ED-IDP and orange dots for ED_EDP).

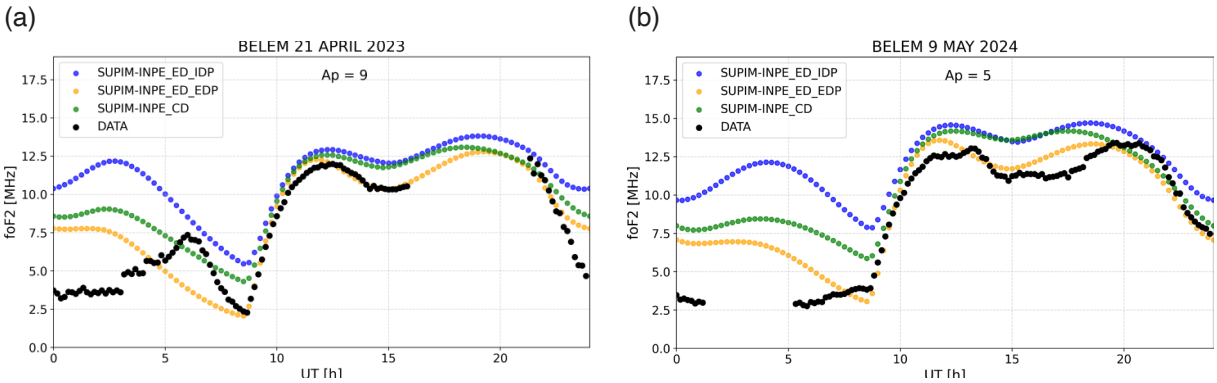


**Figure 1.** foF2 vs UT for Belém, 21 April 2023 (a) and 9 May 2024 (b). SUPIM-INPE ED_IDP (blue dots), SUPIM-INPE ED_EDP (orange dots), SUPIM-INPE CD (green dots) and DATA (black dots).

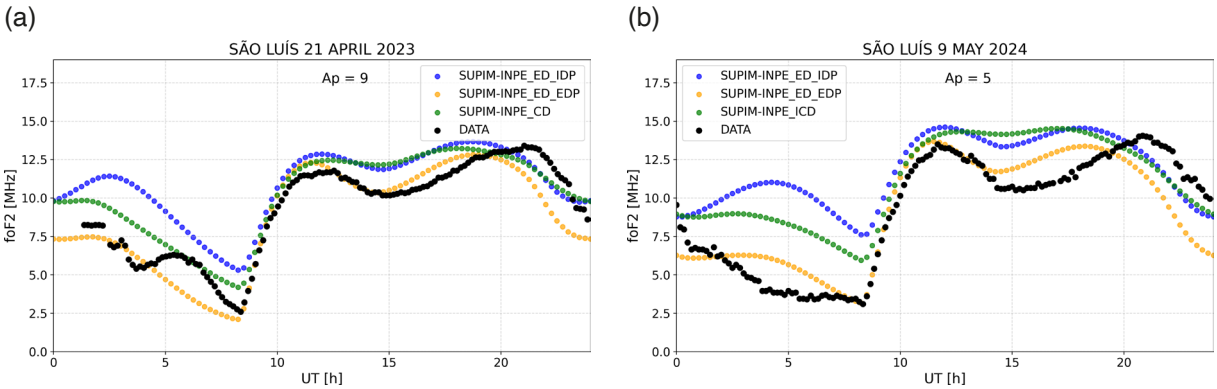


**Figure 2.** foF2 vs UT for São Luís, 21 April 2023 (a) and 9 May 2024 (b). SUPIM-INPE ED_IDP (blue dots), SUPIM-INPE ED_EDP (orange dots), SUPIM-INPE CD (green dots) and DATA (black dots).

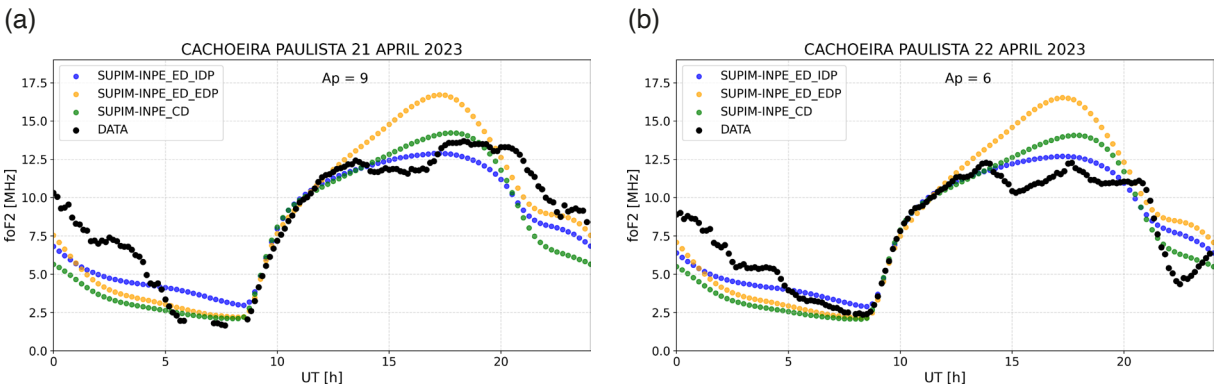


**Figure 3.** foF2 vs UT for Cachoeira Paulista, 21 April 2023 (a) and 22 April 2023 (b). SUPIM-INPE ED_IDP (blue dots), SUPIM-INPE ED_EDP (orange dots), SUPIM-INPE CD (green dots) and DATA (black dots).

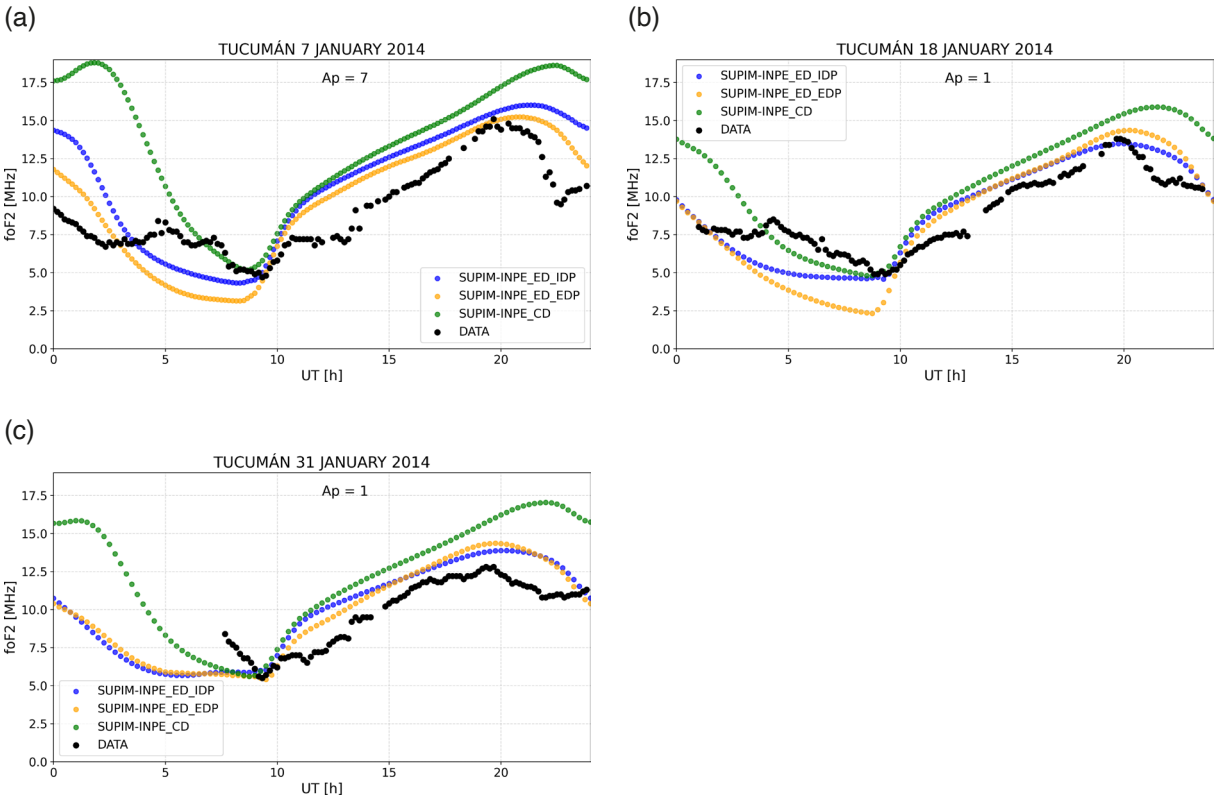


**Figure 4.** foF2 vs UT for Tucumán, 7 January 2014 (a), 18 January 2014 (b) and 31 January 2014 (c). SUPIM-INPE ED_IDP (blue dots), SUPIM-INPE ED_EDP (orange dots), SUPIM-INPE CD (green dots) and DATA (black dots).

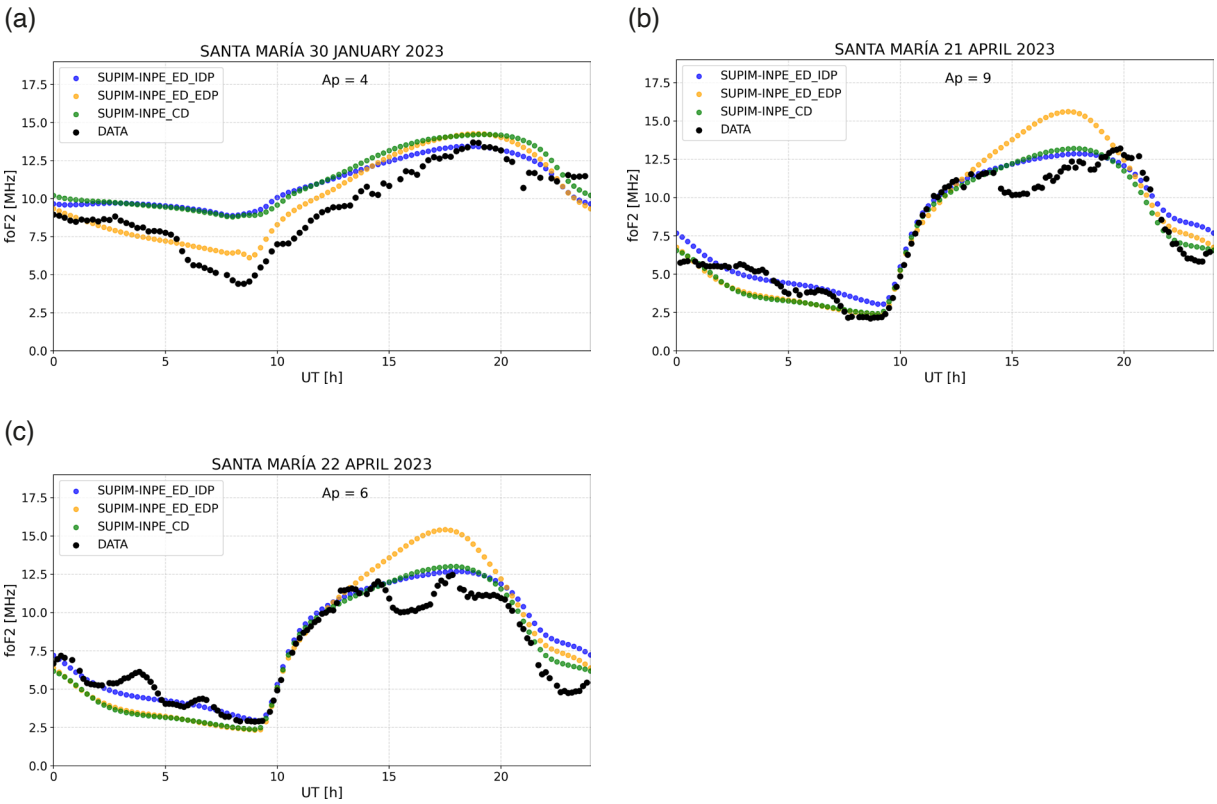


**Figure 5.** foF2 vs UT for Santa Maria, 30 January 2023 (a), 21 April 2023 (b) and 22 April 2023 (c). SUPIM-INPE ED_IDP (blue dots), SUPIM-INPE ED_EDP (orange dots), SUPIM-INPE CD (green dots) and DATA (black dots).

The comparative metrics for each case here analyzed are listed in Table 2. For a clearer visualization of the results, Fig. 6 displays the same information graphically.

**Table 2.** Comparison of MAE, MRE and $R^2$ for SUPIM-INPE models at different stations and dates.

| Stations | Dates | SUPIM-INPE ED_IDP | | | SUPIM-INPE ED_EDP | | | SUPIM-INPE CD | | |
|---|---|---|---|---|---|---|---|---|---|---|
| | | MAE (MHz) | MRE (%) | $R^2$ | MAE (MHz) | MRE (%) | $R^2$ | MAE (MHz) | MRE (%) | $R^2$ |
| Belém | 21 Apr 2023 | 3.1 | 64 | −0.73 | 1.3 | 28 | 0.57 | 1.9 | 40 | 0.33 |
| | 9 May 2024 | 3.7 | 89 | 0.06 | 1.5 | 35 | 0.87 | 2.5 | 58 | 0.59 |
| São Luís | 21 Apr 2023 | 2.0 | 29 | 0.48 | 1.0 | 12 | 0.81 | 1.2 | 16 | 0.78 |
| | 9 May 2024 | 3.1 | 56 | 0.05 | 1.3 | 16 | 0.79 | 2.4 | 40 | 0.47 |
| Cachoeira Paulista | 21 Apr 2023 | 1.3 | 18 | 0.78 | 1.6 | 18 | 0.62 | 1.6 | 20 | 0.58 |
| | 22 Apr 2023 | 1.1 | 16 | 0.83 | 2.0 | 26 | 0.39 | 1.5 | 21 | 0.67 |
| Tucumán | 7 Jan 2014 | 2.6 | 30 | −0.07 | 2.1 | 26 | 0.78 | 4.4 | 52 | −2.86 |
| | 18 Jan 2014 | 1.4 | 17 | 0.60 | 1.9 | 24 | 0.18 | 2.2 | 25 | −0.11 |
| | 31 Jan 2014 | 1.5 | 16 | 0.46 | 1.3 | 14 | 0.52 | 2.8 | 29 | −1.26 |
| Santa Maria | 30 Jan 2023 | 1.7 | 25 | 0.27 | 1.1 | 14 | 0.77 | 2.0 | 26 | 0.27 |
| | 21 Apr 2023 | 1.4 | 17 | 0.91 | 0.8 | 14 | 0.73 | 0.9 | 13 | 0.91 |
| | 22 Apr 2023 | 0.9 | 14 | 0.83 | 1.6 | 22 | 0.55 | 1.1 | 17 | 0.82 |

In equatorial regions, such as Belém (1.45°S, 48.48°W) and São Luís (2.52°S, 44.30°W), shown in Figs. 1 and 2, respectively, foF2 variability is primarily governed by the equatorial vertical E×B drift. Under moderate solar activity conditions (21 April 2023), the ED_EDP configuration reproduces the equatorial plasma depletion more accurately than CD between 0 and 5 UT, as well as around the foF2 minimum. This improvement is reflected mainly in reduced errors and slightly higher $R^2$, as can be noticed in Fig. 6. During the period of higher solar activity (9 May 2024), the ED_EDP model maintains low errors and a high $R^2$. In contrast, the ED_IDP version exhibits the largest errors and lowest $R^2$ values, indicating increased sensitivity to numerical truncation effects near the magnetic equator.

At low magnetic latitude stations such as Cachoeira Paulista (22.65°S, 45.00°W; Fig. 3) and Tucumán (26.90°S, 65.40°W; Fig. 4), foF2 behavior is primarily controlled by plasma transport from the equator along magnetic field lines. The ED_IDP configuration shows overall better agreement on 21 and 22 April 2023 for Cachoeira Paulista, whereas ED_EDP and CD perform worse. In particular, on 22 April, CD shows intermediate performance, while ED_EDP performs worst. This indicates that the representation of the magnetic field geometry and the associated plasma transport pathways can be more critical than numerical precision alone in reproducing foF2 variability at low magnetic latitudes.

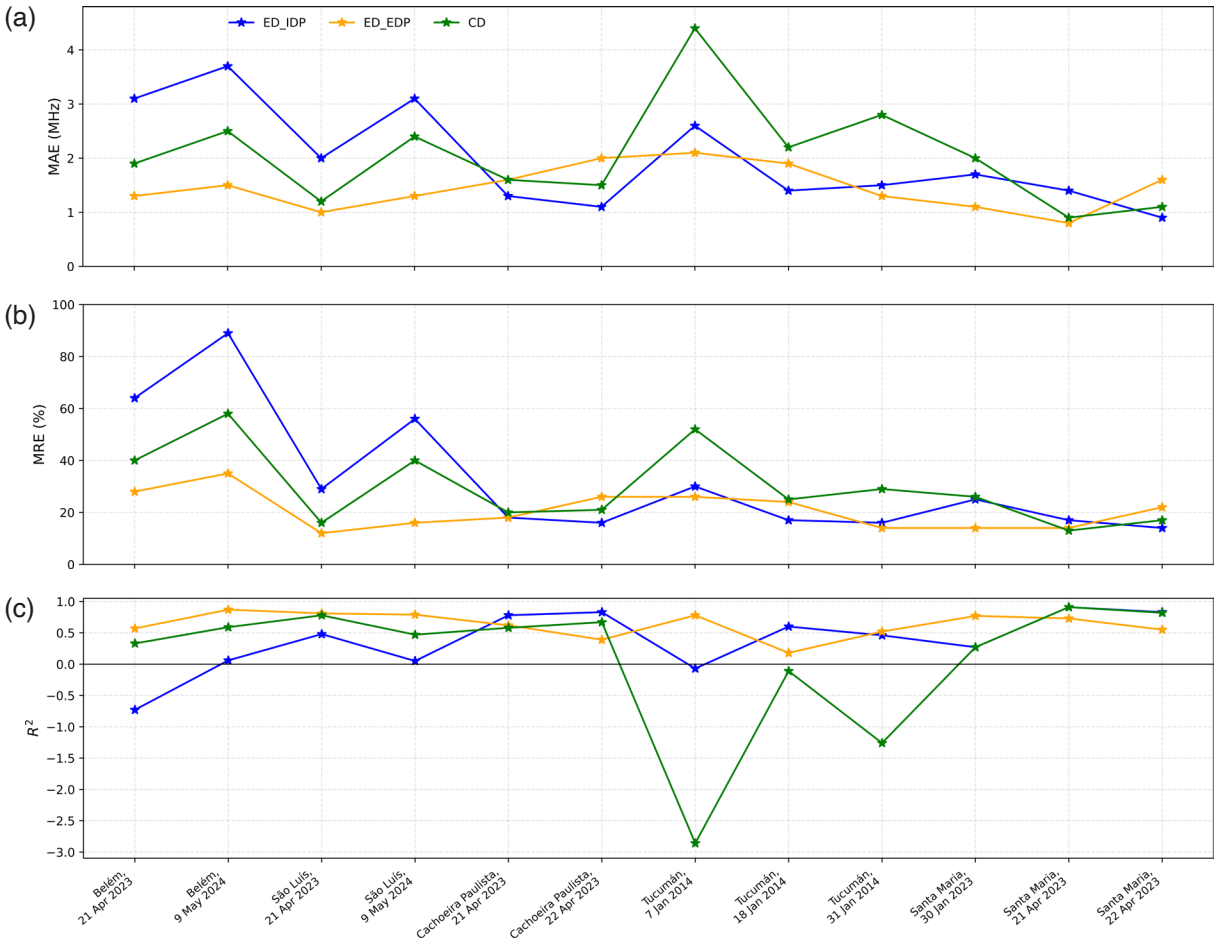


**Figure 6.** MAE (a), MRE (b) and $R^2$ (c) of each station and case listed in Table 2 and for each model configuration: SUPIM-INPE ED_IDP (blue), SUPIM-INPE ED_EDP (orange) and SUPIM-INPE CD (green).

For Tucumán station, ED_EDP exhibits clear improvements on 7 and 31 January 2014, with higher $R^2$ values and reduced errors, while on 18 January 2014 the ED_IDP configuration shows slightly better performance. This behavior suggests that the relative importance of numerical precision depends on the prevailing geophysical conditions, with double precision becoming more critical during periods of enhanced plasma transport and stronger ionospheric forcing. In addition, Tucumán stands out by presenting multiple negative $R^2$ values, including two values below −1 for the CD configuration. Although a negative $R^2$ value is also obtained at Belém for the ED_IDP configuration, the negative values at Tucumán are more frequent and larger in magnitude. These results indicate that, for those cases, the CD model configuration has no predictive skill relative to the observational mean. The better performance of the ED_EDP configuration when considering $R^2$ values reinforces the importance of both an improved magnetic field representation and enhanced numerical precision for accurately reproducing foF2 variability.

Finally, at the Santa María station (29.68°S, 53.80°W), shown in Fig. 5, also influenced by the Equatorial Ionization Anomaly (EIA), for 30 January 2023, the ED_EDP configuration shows the best overall agreement with observations, in terms of both error metrics and $R^2$. However, this behavior is not consistent across all conditions. For instance, on 21 April, ED_EDP remains the best-performing configuration. However, this is not the case on 22 April, when it becomes the poorest-performing configuration and ED_IDP provides the best results. This indicates that the impact of numerical precision depends on the specific ionospheric conditions, and different configurations may better reproduce different aspects of the observed variability.

Overall, ED_EDP yields the lowest errors and the highest explanatory capability in most cases, particularly at low magnetic latitudes. The CD configuration generally exhibits larger discrepancies and lower $R^2$ values, especially at stations influenced by the EIA, reflecting limitations associated with its simplified magnetic geometry. This can be clearly seen in Fig. 7 which shows the mean values of the comparative metrics here analyzed, averaged over all the cases considered.

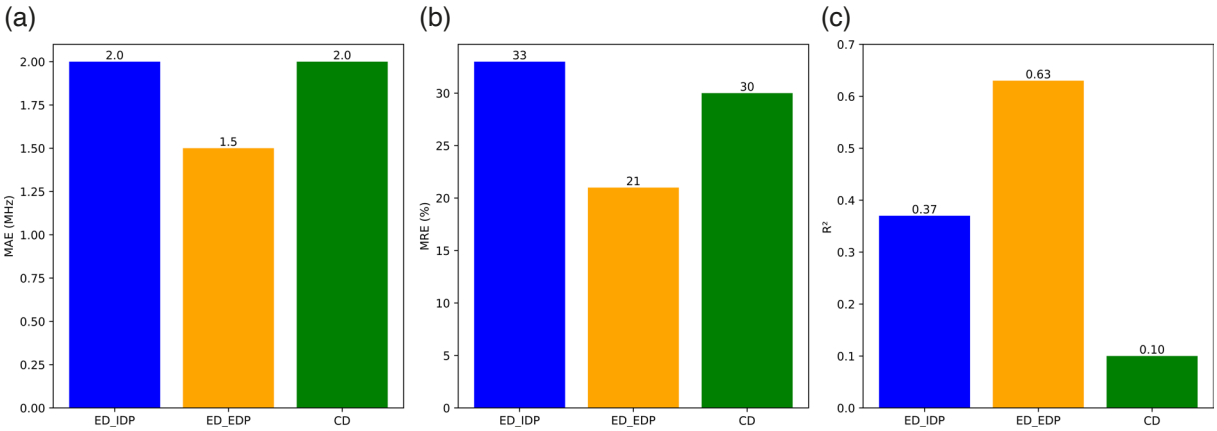


**Figure 7.** MAE (a), MRE (b) and $R^2$ (c) mean values over all analyzed stations and dates, for each model configuration: SUPIM-INPE ED_IDP (blue), SUPIM-INPE ED_EDP (orange) and SUPIM-INPE CD (green).

Figure 8 illustrates the latitudinal structure of the ionosphere for the different model configurations at Tucuman on 7 January 2014, corresponding to the case with the largest discrepancies in $R^2$. Clear differences are observed in the position and intensity of the EIA crests between SUPIM-INPE configurations. In particular, small shifts in the crest location relative to Tucumán location (indicated by the vertical line) lead to significant differences in the local plasma frequency. In fact, the changes in the locations of the crests are consequences of the displacements of the magnetic equator in relation to the geographic equator. This helps explain the variability in foF2 and the differences in model performance among configurations.

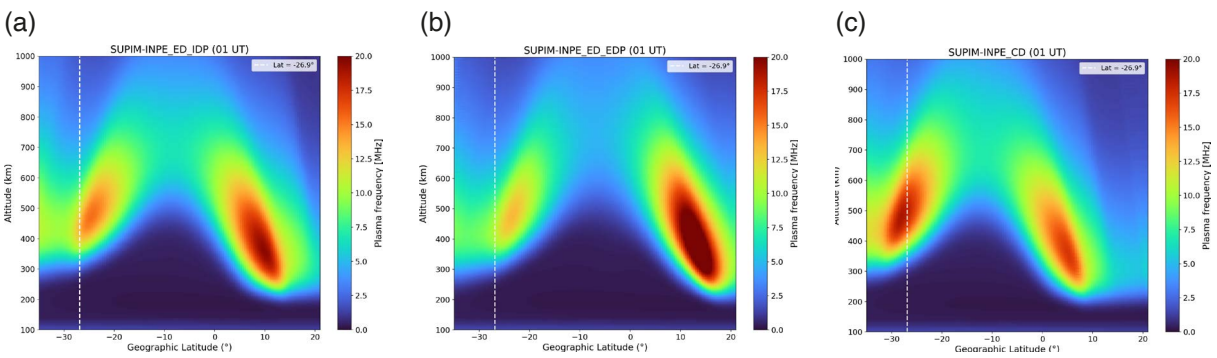


**Figure 8.** Latitude vs. Altitude distribution of plasma frequency at 01:00 UT on 7 January 2014 over Tucumán (Ap = 7), for SUPIM-INPE ED_IDP (a), SUPIM-INPE ED_EDP (b), and SUPIM-INPE CD (c) configurations. The vertical dashed line indicates the geographic latitude of Tucumán (26º90 S).

The discrepancies observed between the SUPIM simulations and the ionospheric measurements, particularly during nighttime, can be attributed to uncertainties in the specification of key driving parameters. The F-region electron density, and consequently foF2, is highly sensitive to the combined effects of vertical plasma drift and thermospheric neutral winds. Small deviations in these inputs may lead to significant differences in the modeled peak density and layer height.

In the present study, the vertical plasma drift was prescribed using an empirical model. However, previous investigations over the Brazilian sector have demonstrated that empirical drift models do not always fully capture the regional electrodynamic variability, even under geomagnetically quiet conditions. This limitation is particularly relevant over low-latitude South America, where the large magnetic declination angle and the influence of the SAMA modify the coupling between neutral winds, electric fields, and plasma transport. As a result, the actual vertical E×B drift may deviate from the climatological pattern assumed by the model.

Similarly, the neutral wind field specified by HWM14 may not fully reproduce the regional and temporal variability of thermospheric dynamics over Brazil. Since meridional winds strongly control the plasma redistribution along

magnetic field lines, inaccuracies in their representation can directly affect the simulated F-region peak density and height, especially after sunset when electrodynamic control becomes more sensitive to background conditions.

On the other hand, the neutral composition and temperature provided by NRLMSISE-00 generally reproduce large-scale climatological behavior; however, localized or short-term deviations from climatology can not be captured. Therefore, the combined uncertainties in electric fields and neutral winds, together with the intrinsic limitations of empirical background models, likely explain the differences between the SUPIM results and the observations.

## 4. Conclusions

This study evaluated the performance of the SUPIM-INPE model in reproducing foF2 values under geomagnetically quiet conditions using observations from five stations in South America. The analysis demonstrates that the foF2 modeled value is influenced by both the magnetic field geometry and the numerical precision adopted in the model. According to the comparative metrics listed in Table 2 and shown in Fig. 6, together with their mean values shown in Fig. 7, the ED_EDP configuration provides the best overall representation of foF2 under the conditions considered in this study. These results indicate that the use of explicit double precision within the ED magnetic field framework generally improves the model's capability to reproduce the observed foF2 variability. That is, the superior performance of ED_EDP suggests that the benefits of the ED geomagnetic representation can be fully realized when the associated coordinate transformations and field-line calculations are performed with sufficient numerical precision.

Under disturbed geomagnetic conditions, enhanced variability in electrodynamic and thermospheric processes may introduce additional complexities, making it more difficult to unambiguously assess the specific impact of the magnetic field configuration.

The discrepancies between the SUPIM simulations and observational data highlight the intrinsic limitations of empirical background models (such as those used for plasma drift, neutral winds, and composition) in capturing the complex, short-term regional electrodynamics unique to the South American sector, particularly under the influence of the large magnetic declination, the SAMA and the EIA.

Overall, these findings highlight that both an improved representation of the geomagnetic field and enhanced numerical precision are essential for reliable ionospheric modeling of foF2. Future work will extend this evaluation to additional regions and geomagnetic conditions to further assess the robustness of the ED configuration.

**Data availability statement.** The data used in this work were obtained from Tucuman Station, whose page is: https://spaceweather.facet.unt.edu.ar/monitoreo/. The Digisonde data from Belém, Cachoeira Paulista, São Luís and Santa María can be downloaded upon registration at the Embrace webpage from INPE Space Weather Program in the following link: http://www2.inpe.br/climaespacial/portal/en/.

**Acknowledgments.** J. R. Souza and A. M. Santos would like to thank the Brazilian Ministry of Science, Technology and Innovation (MCTI), the Brazilian Space Agency (AEB) and INPE. JRS also thanks to CNPq (Grant 311840/2022-1) and Fundação de Amparo à Pesquisa do Estado de São Paulo (FAPESP) through the project 2021/07206-0. M. Bravo acknowledges the ANID SUBDIRECCIÓN DE INVESTIGACIÓN APLICADA/ID25I10556.

## References

Abdu, M. A., S. Ananthakrishnan, E. F Coutinho, B. A. Krishnan and E. M. D. S. Reis (1973). Azimuthal drift and precipitation of electrons into the South Atlantic geomagnetic anomaly during an SC magnetic storm, J. Geophy. Res., 78, 25, 5830-5836, doi:10.1029/JA078i025p05830.

Abdu, M. A., I. S. Batista, A. J. Carrasco and C. G. M. Brum (2005). South Atlantic magnetic anomaly ionization: A review and a new focus on electrodynamic effects in the equatorial ionosphere, J. Atmo. Solar-Terres. Phys., 67, 17-18, 1643-1657, doi:10.1016/j.jastp.2005.01.014.

Abdu, M., J. H. A. Sobral, O. R. Nelson and I. S. Batista (1985). Solar cycle related range-type spread-F occurrence characteristics over equatorial and low-latitude stations in Brazil, J. Atmo. Terres. Phys., 47, 8-10, 901-905, doi:10.1016/0021-9169(85)90065-0.

Bailey, G. J. and R. Sellek (1990). A mathematical model of the Earth's plasmasphere and its application in a study of $He^+$ at L = 3.0, Ann. Geophysicae, 8, 171-190.

Bailey, G. J., R. Sellek and N. Balan (1993). A modelling study of the equatorial topside ionosphere, Ann. Geophysicae, 11, 263-272.

Bailey, G. J. and N. Balan (1996). A low-latitude ionosphere-plasmasphere model. In R. W. Schunk (Ed.), STEP handbook on ionospheric models, 173-206, Utah State University.

Bailey, G. J., Y. Z. Su and N. Balan (1997). The Sheffield University plasmasphere-ionosphere model: A review. J. Atmo. Terres. Phys., 59, 1541-1552.

Batista, I. S. and A. M. Abdu (1977). Magnetic storm associated delayed sporadic enhancements in the Brazilian geomagnetic anomaly, J. Geophys. Res., 82, 29, 4777-4783, doi:10.1029/JA082i029p04777.

Cole, K. D. (1963). Eccentric dipole coordinates, Australian Journal of Physics, 16, 423-429.

Da Silva, L. A., J. Shi, L. C. A. Resende, O. V. Agapitov et al. (2022). The role of inner radiation belt dynamics in the generation of auroral-type sporadic E layers over the South American magnetic anomaly, Front. Astron. Space Sci., 9, 970308, doi:10.3389/fspas.2022.970308.

Drob, D. P., J. T. Emmert, J. W. Meriwether, J. J. Makela, E. Doornbos et al. (2015). An update to the Horizontal Wind Model (HWM): The quiet-time thermosphere, Earth and Space Science, 2, 301-319, doi:10.1002/2014EA000089.

Fraser-Smith, A. C. (1987). Centered and eccentric geomagnetic dipoles and their poles, 1600-1985, Rev. Geophys., 25, 1, 1-16.

Huba, J. D., G. Joyce and J. A Fedder (2000). Sami2 is Another Model of the Ionosphere (SAMI2): A new low-latitude ionosphere model, J. Geophys. Res., 105, A10, 23,035-23,053, doi:10.1029/2000JA000035.

Koochak, Z. and A. C. Fraser-Smith (2017). An update on the centered and eccentric geomagnetic dipoles and their poles for the years 1980-2015, Earth and Space Science, 4, 407-429, doi:10.1002/2017EA000280.

Lomotey, S. O., J. R. de Souza, C. M. Wrasse, H. Takahashi, D. Barros, C. A. O. B. Figueiredo et al. (2024). Variability of the equatorial ionization anomaly over the South American sector: Effects of electric field and effective meridional wind, J. Atmo. Solar-Terres. Phys., 106499, doi:10.1016/j.jastp.2024.106499.

Molina, M. G., M. Cabrera, R. Ezquer, P. Fernandez and E. Zuccheretti (2013). Digital signal processing and numerical analysis for radar in geophysical applications, Adv. Space Res., 51, 1870-1877, doi:10.1016/j.asr.2012.07.032.

Picone, J. M., A. E. Hedin, D. P. Drob and A. C. Aikin (2002). NRLMSISE-00 empirical model of the atmosphere: Statistical comparisons and scientific issues, J. Geophys. Res., 107, A12, 1468, doi:10.1029/2002JA009430.

Reinisch, B. W., I. A. Galkin, G. M. Khmyrov, A. Kozlov et al. (2009). New Digisonde for research and monitoring applications, Radio Sci., 44, 1, RS0A24, doi:10.1029/2008rs004115.

Reinisch, B. W. and X. Huang (1983). Automatic Calculation of Electron Density Profiles from Digital Ionograms: 3. Processing of Bottomside Ionograms, Radio Sci., 18, 3, 477-492, doi:10.1029/RS018i003p00477.

Reinisch, B. W., X. Huang, V. Galkin, V. Paznukhov and A. Kozlov (2005). Recent advances in real-time analysis of ionograms and ionospheric drift measurements with digisondes, J. Atmos. Solar-Terr. Physics, 67, 1054-1062. doi:10.1016/j.jastp.2005.01.009.

Resende, L. C. A., Y. Zhu, A. M. Santos, R. A. J. Chagas et al. (2024). Nocturnal sporadic cusp-type layer resulting from anomalous excess ionization over the SAMA region during the extreme magnetic storm of May 11, 2024, J. Geophys. Res.: Space Physics, 129, e2024JA033167, doi:10.1029/2024JA033167.

Richards, P. G., T. N. Woods and W. K. Peterson (2006). HEUVAC: A new high resolution solar EUV proxy model, Adv. Space Res., 37, 2, 315-322, doi:10.1016/j.asr.2005.06.031.

Richards, P. G., R. R. Meier and P. J. Wilkinson (2010). On the consistency of satellite measurements of thermospheric composition and solar EUV irradiance with Australian ionosonde electron density data, J. Geophys. Res.: Space Phys., 115, A10, doi:10.1029/2010JA015368.

Santos, P. M. T., J. R. Souza., J. H. A. Sobral, G. J. Bailey and C. G. M. Brum (2005). Development of the Sheffield University Plasmasphere Ionosphere Model-Enhanced (SUPIM-E). In Proceedings of the 2005 CEDAR-GEM Joint Workshop.

Santos, A. M., M. A. Abdu, J. R. Souza, J. H. A. Sobral and I. S. Batista (2016a). Disturbance zonal and vertical plasma drifts in the Peruvian sector during solar minimum phases, J. Geophys. Res.: Space Phys., 121, 2503-2521, doi:10.1002/2015JA022146.

Santos, A. M., M. A. Abdu, J. R. Souza, A. Sobral et al. (2016b). Storm time equatorial plasma bubble zonal drift reversal due to disturbance Hall electric field over the Brazilian region, J. of Geophys. Res.: Space Physics, 121, 6, 5594-5612, doi:0.1002/2015JA022179.

Scherliess, L. and B. G. Fejer (1999). Radar and satellite global equatorial F-region vertical drift model, J. Geophys. Res., 104, A4, 6829-6842.

Schmidt, A. (1934). Der magnetische Mittelpunkt der Erde und seine Bedeutung, Gerlands Beiträge zur Geophysik, 41, 346-358.

Souza, J. R., M. Abdu, I. Batista and G. Bailey (2000). Determination of vertical plasma drift and meridional wind using the Sheffield University Plasmasphere Ionosphere Model and ionospheric data at equatorial and low latitudes in Brazil: Summer solar minimum and maximum conditions, J. Geophys. Res.: Space Phys., 105, A6, 12813-12821.

Souza, J. R., C. G. M. Brum, M. A. Abdu, I. S. Batista et al. (2010). Parameterized regional ionospheric model and comparison with experimental data and IRI representations. Adv.Space Res., 46, 1032-1038.

Souza, J. R., W. D. Asevedo Jr., P. C. P. dos Santos, A. Petry et al. (2013). Longitudinal variation of the equatorial ionosphere: modeling and experimental results, Adv.Space Res., 51, 4, 654-660, doi:10.1016/j.asr.2012.01.023.

Zuccheretti, E., G. Tutone, U. Sciacca, C. Bianchi and J. A. Baskaradas (2003). The new AIS-INGV digital ionosonde. Ann. Geophys, 46, 4, 647-659. doi:10.4401/ag-4377.

***CORRESPONDING AUTHOR: Valentín VENCHIARUTTI**,
Universidad Nacional de Tucumán, Facultad de Ciencias Exactas y Tecnología, Departamento de Física, Tucumán, Argentina
e-mail:vvenchiarutti@herrera.unt.edu.ar

© 2026 the Author(s).
Open Access. This article is licensed under a Creative Commons Attribution 4.0 International License